



Regerite, $\text{KFe}_6(\text{PO}_4)_4(\text{OH})_7(\text{H}_2\text{O})_6 \cdot 4\text{H}_2\text{O}$, the first new mineral species from the Kreuzberg pegmatite, Pleystein, Oberpfalz, Bavaria, Germany

Christian Rewitzer¹, Rupert Hochleitner², Ian E. Grey³, Anthony R. Kampf⁴, Stephanie Boer⁵, and Colin M. MacRae³

¹private address: Graf von Bogen Str. 6, 93437 Furth im Wald, Germany

²Mineralogical State Collection (SNSB), Theresienstraße 41, 80333 Munich, Germany

³CSIRO Mineral Resources, Private Bag 10, Clayton South, Victoria 3169, Australia

⁴Mineral Sciences Department, Natural History Museum of Los Angeles County,
900 Exposition Boulevard, Los Angeles, CA 90007, USA

⁵Australian Synchrotron, ANSTO, 800 Blackburn Road, Clayton, Victoria 3168, Australia

Correspondence: Ian E. Grey (ian.grey@csiro.au)

Received: 20 July 2023 – Revised: 17 August 2023 – Accepted: 18 August 2023 – Published: 25 September 2023

Abstract. Regerite, $\text{KFe}_6(\text{PO}_4)_4(\text{OH})_7(\text{H}_2\text{O})_6 \cdot 4\text{H}_2\text{O}$, is the first new mineral species to be characterised from the Kreuzberg pegmatite, Pleystein, in the Oberpfalz, Bavaria. It was found in vugs on a specimen of drusy quartz, associated with rockbridgeite, strengite and phosphosiderite. Regerite occurs as clusters of yellowish-green prisms, typically 5 to 20 μm wide and up to 0.1 mm long. The crystals are flattened on {100} and elongated along [001], and they display the forms {100}, {010} and {011}. The measured density is $2.69(2) \text{ g cm}^{-3}$. Optically, regerite crystals are biaxial (+), with $\alpha = 1.670(5)$, $\beta = 1.690(5)$ and $\gamma = 1.730(5)$ (measured in white light), and $2V$ (meas) is $76(2)^\circ$. The empirical formula from electron microprobe analyses and crystal structure refinement is $\text{K}_{0.95}(\text{Fe}_{5.66}^{3+}\text{Ti}_{0.45})_{\Sigma 6.11}(\text{PO}_4)_{3.95}(\text{OH})_7[(\text{H}_2\text{O})_{5.33}(\text{OH})_{0.88}]_{\Sigma 6.21} \cdot 4\text{H}_2\text{O}$. Regerite has monoclinic symmetry, with space group $P2_1/c$ and unit-cell parameters $a = 15.408(11) \text{ \AA}$, $b = 17.311(11) \text{ \AA}$, $c = 9.870(11) \text{ \AA}$, $\beta = 95.42(2)^\circ$, $V = 2621(3) \text{ \AA}^3$ and $Z = 4$. The crystal structure was refined using synchrotron single-crystal data to $wR_{\text{obs}} = 0.065$ for 6088 reflections with $I > 3\sigma(I)$. The structure type has not been previously reported. It is made of heteropolyhedral layers parallel to {100} that consist of Fe-centred octahedra and PO_4 tetrahedra. The layers are interconnected via edge-shared octahedral dimers to form slit-like channels along [001] that are occupied by K^+ ions and water molecules.

1 Introduction

The Kreuzberg pegmatite is a zoned pegmatite body intruded into Variscan biotite gneisses. It can be considered a pegmatitic rest differentiate of the upper Carboniferous Flossenbürg granite (Fischer, 1965). The pegmatite is heavily eroded with the quartz core left as a free-standing quartz rock with a height of about 25 m in the middle of the town of Pleystein (Fig. 1). A cloister is situated on top of the rock. From 1851 to 1920, the quartz was quarried as raw material for the porcelain and glass industry. Since 1920, quarrying was forbidden as it threatened the town's landmark. During the quar-

rying period, many phosphates, especially crystals of strengite and phosphosiderite up to more than 1 cm in length, were found in druses in the quartz. Later, similar finds were made in 1951 during construction work and after a large rockfall (Wilk, 1967). Mindat records 58 valid mineral species from the pegmatite but no type minerals. Today, the rock is under nature protection, and new finds of phosphates are not possible at the site. The specimen containing regerite was collected during the 1950s and acquired by Christian Rewitzer for his private collection. During a recent study of minerals from the collection using energy-dispersive X-ray analysis,



Figure 1. Rose quartz residual core of Kreuzberg pegmatite at Pleystein, with a cloister on top. Photo by Rupert Hochleitner.

co-authors Christian Rewitzer and Rupert Hochleitner identified regerite as a potential new secondary phosphate mineral based on its composition, which includes the relatively rare element Ti in association with K and Fe. The new species and its name were approved by the International Mineralogical Association (IMA) Commission on New Minerals, Nomenclature and Classification (CNMNC), IMA-2023-028.

The name honours the married couple Grete (born 25 September 1948) and Werner (born 4 June 1946) Reger from Pleystein. The couple manage the Stadtmuseum at Pleystein and show immense dedication to make known the minerals of Kreuzberg and Hagendorf to the public. Without them, the famous Lehner collection, the most extensive collection of historical Kreuzberg mineral samples on display, would not be known to scientists and collectors. That there is now the most comprehensive collection of Hagendorf phosphates open to the public in the Pleystein museum is, to a great extent, due to their efforts. The holotype specimen is housed in the collections of the Mineralogical State Collection Munich (SNSB); the registration number is MSM 38039. A cotype used for optical characterisation, Raman spectroscopy and the powder diffraction pattern is housed in the mineralogical collections of the Natural History Museum of Los Angeles County, catalogue number 76299.

2 Occurrence and associated minerals

The specimen containing regerite comes from the Kreuzberg pegmatite, Pleystein, in the Oberpfalz, northeastern Bavaria ($49^\circ 38' 47''$ N, $12^\circ 24' 42''$ E). The specimen consists of drusy quartz with rockbridgeite as the principal cavity-filling mineral. Crystals of strengite and phosphosiderite are also present in cavities. Yellowish-green prisms of regerite are

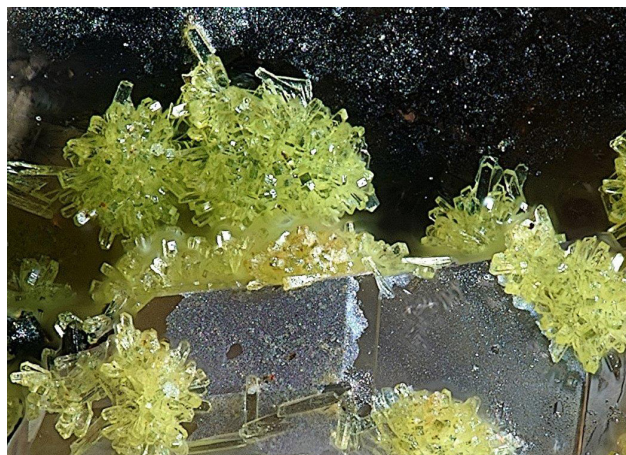


Figure 2. Yellowish-green regerite crystals on strengite on the holotype specimen (MSM 38039). Photo by Christian Rewitzer. Field of view: 0.25 mm across.

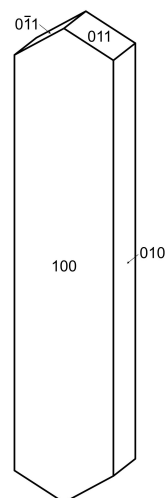


Figure 3. Crystal drawing of regerite: clinographic projection.

found in the cavities, sometimes growing on strengite crystals, and thus they are younger than strengite.

3 Physical and optical properties

Regerite forms clusters of yellowish-green prisms with chisel-shaped terminations (Fig. 2), having cross-sections of typically 5 to 20 μm and up to 100 μm long. The crystals are flattened on {100} and elongated along [001], and they display the forms {100}, {010} and {011} (Fig. 3). The density measured by flotation in a mixture of methylene iodide and toluene is $2.69(2) \text{ g cm}^{-3}$, which compares with a calculated density of 2.66 g cm^{-3} for the empirical formula and unit-cell volume refined from single-crystal XRD data.

Optically, regerite crystals are biaxial (+), with $\alpha = 1.670(5)$, $\beta = 1.690(5)$ and $\gamma = 1.730(5)$ (measured in

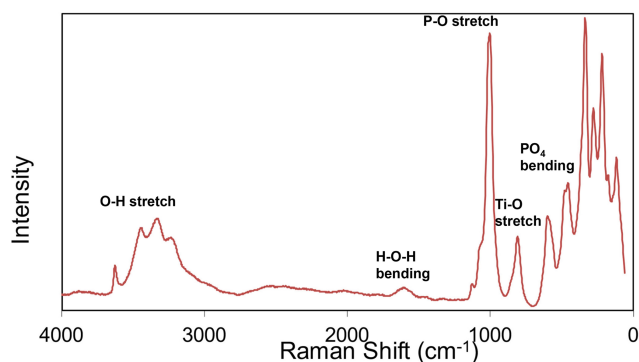


Figure 4. Raman spectrum for regerite.

Table 1. Chemical data (wt %) for regerite.

Constituent	Mean	Range	SD	Standard
K_2O	4.28	3.85–4.66	0.26	adularite
Fe_2O_3	43.1	41.9–43.7	0.6	hematite
TiO_2	3.41	2.17–4.26	0.58	rutile
P_2O_5	26.7	25.1–28.9	1.1	berlinite
H_2O^*	22.8			
Total	100.29			

* Based on the crystal structure (see text).

white light). The measured $2V$ from extinction data analysed with EXCALIBR (Gunter et al., 2004) is $76(2)^\circ$, and the calculated $2V$ is 72.0° . Dispersion and pleochroism were not observed. The optical orientation is $Y = b$, $Z^{\wedge}c \approx 10^\circ$.

4 Chemical composition

Crystals of regerite were analysed using wavelength-dispersive spectrometry on a JEOL JXA 8500F Hyperprobe operated at an accelerating voltage of 15 kV and a beam current of 2 nA. The beam was defocused to 5 μm . Analytical results (average of analyses on 15 crystals) are given in Table 1. There was insufficient material for direct determination of H_2O , whose presence is confirmed by the low analysis total for oxides and by Raman spectroscopy. The calculated H_2O was based upon the ideal formula from the crystal structure (27 H atoms), decreased by the Ti content (0.44 apfu) according to $\text{Ti}^{4+} + (\text{OH})^- \rightarrow \text{Fe}^{3+} + \text{H}_2\text{O}$. The empirical formula based on $\text{O} = 33$ is $\text{K}_{0.95}(\text{Fe}_{5.66}^{3+}\text{Ti}_{0.45})_{\Sigma 6.11}(\text{PO}_4)_{3.95}(\text{OH})_7[(\text{H}_2\text{O})_{5.33}(\text{OH})_{0.88}]_{\Sigma 6.21} \cdot 4\text{H}_2\text{O}$.

The simplified formula is $\text{K}(\text{Fe}^{3+}, \text{Ti}^{4+})_6(\text{PO}_4)_4(\text{OH})_7(\text{H}_2\text{O}, \text{OH})_6 \cdot 4\text{H}_2\text{O}$.

The ideal formula is $\text{KFe}_6(\text{PO}_4)_4(\text{OH})_7(\text{H}_2\text{O})_6 \cdot 4\text{H}_2\text{O}$, which requires K_2O 4.47, Fe_2O_3 45.48, P_2O_5 26.95, H_2O 23.1, total 100 wt %.

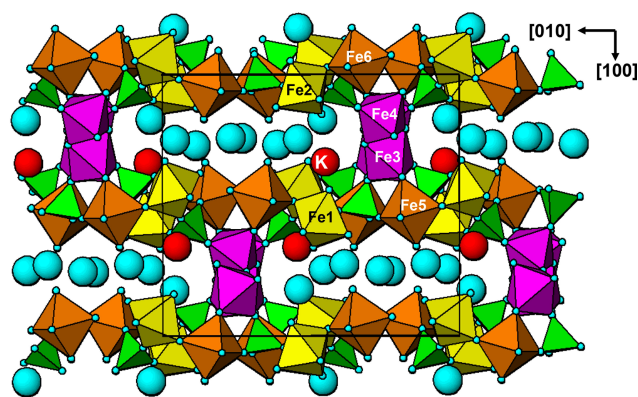


Figure 5. [001] projection of the structure of regerite. Large blue spheres are water molecules.

5 Raman spectroscopy

Raman spectroscopy was conducted on a Horiba XploRA PLUS spectrometer using a 532 nm diode laser, 100 μm slit, 1800 g mm^{-1} diffraction grating and a $100 \times (0.9 \text{ NA})$ objective. The spectrum is shown in Fig. 4. The O–H stretch region has a broad band that can be assigned to H-bonded water, with three maxima at 3445, 3325 and 3230 cm^{-1} . A weak sharp band at 3625 cm^{-1} is most likely due to hydroxyls. The H–O–H bending mode region for water has a peak at 1610 cm^{-1} . The P–O stretching region has a strong band at 1005 cm^{-1} with a shoulder at 1075 cm^{-1} , corresponding to symmetric P–O stretching modes, together with a weak band at 1130 cm^{-1} due to antisymmetric P–O stretching. Bending modes of the $(\text{PO}_4)^{3-}$ groups are manifested by two bands centred at 590 and 470 cm^{-1} . Peaks at lower wavenumbers are related to lattice vibrations. A band at 805 cm^{-1} is assigned as a Ti–O stretch vibration by analogy with the Raman spectra for Ti-bearing paulkerrite-group minerals (Grey et al., 2023) and titanates that have chains of Ti-centred octahedra with relatively short ($\sim 1.8 \text{ \AA}$) Ti–O bonds (Tu et al., 1996; Bamberger et al., 1990; Silva et al., 2018). This implies that the Ti atoms substituting at the Fe sites in the short-chain octahedra in the structure are displaced from the octahedral centres to give short Ti–O distances.

6 Crystallography

X-ray powder diffraction data were recorded using a Rigaku R-Axis RAPID II curved imaging plate microdiffractometer with monochromatised Mo $K\alpha$ radiation. A Gandolfi-like motion on the ϕ and ω axes was used to randomise the sample. Observed d values and intensities were derived by profile fitting using JADE Pro software (Materials Data, Inc.). Data are given in Table 2. Unit-cell parameters refined from the powder data using JADE Pro with whole pattern fitting are as follows: $a = 15.408(11) \text{ \AA}$, $b = 17.311(11) \text{ \AA}$,

Table 2. Powder X-ray data (d in Å) for regerite compared to that calculated from the structure. Only calculated lines with $I \geq 1.5$ are listed*.

I_{obs}	d_{obs}	d_{calc}	I_{calc}	hkl	I_{obs}	d_{obs}	d_{calc}	I_{calc}	hkl	I_{obs}	d_{obs}	d_{calc}	I_{calc}	hkl
63	11.52	11.4708	67	1 1 0	6	2.583	2.6116	3	-1 4 3	12	1.8357	1.8441	4	-2 9 1
10	8.72	8.6755	8	0 2 0			2.5819	2	-4 1 3			1.8297	10	6 3 3
		8.5629	3	0 1 1	21	2.543	2.5488	13	1 4 3			1.8128	2	-8 3 1
100	7.69	7.6442	100	2 0 0			2.5359	10	-3 5 2			1.7758	4	2 3 5
7	6.10	5.9428	7	-2 1 1	13	2.479	2.4934	6	0 6 2	7	1.7446	1.7488	3	8 4 0
20	5.85	5.8621	11	1 2 1			2.4714	6	5 1 2			1.7374	7	-3 4 5
		5.7354	8	2 2 0			2.4637	3	-3 6 1	18	1.7050	1.7112	3	-3 9 2
12	5.42	5.4095	11	1 3 0			2.4549	2	-5 3 2			1.7052	5	-7 1 4
16	4.93	4.9227	10	0 0 2			2.4413	2	-1 1 4			1.7012	2	-1 10 1
		4.8896	7	3 1 0	18	2.413	2.4245	5	3 5 2			1.6906	9	9 1 0
8	4.65	4.6409	10	-1 1 2			2.4082	11	-2 0 4			1.6862	2	-3 7 4
18	4.41	4.4150	20	1 1 2			2.4005	4	-3 4 3	15	1.6411	1.6500	3	-8 3 3
		4.3378	2	0 4 0	4	2.372	2.3802	3	5 4 1			1.6457	2	-9 1 2
18	4.28	4.2683	18	-2 3 1			2.3526	2	-6 0 2			1.6387	7	7 7 0
13	3.968	3.9761	12	2 0 2			2.3206	2	-2 5 3			1.6354	3	-2 0 6
33	3.877	3.8995	11	3 2 1	6	2.291	2.2942	3	5 5 0			1.6308	4	5 9 0
		3.8772	22	-1 4 1			2.2826	4	2 0 4	10	1.6121	1.6202	3	3 7 4
28	3.797	3.8081	28	1 4 1			2.2682	2	-1 3 4			1.6124	2	3 10 1
		3.7727	7	2 4 0	17	2.234	2.2275	14	6 3 1			1.6089	3	2 9 3
16	3.662	3.7011	5	-1 3 2			2.2134	2	1 3 4	7	1.5850	1.5903	3	2 10 2
		3.6325	14	-3 1 2			2.2043	2	4 3 3			1.5830	4	-9 4 1
		3.5986	2	-4 1 1	11	2.159	2.1615	8	-4 0 4			1.5708	2	-6 3 5
16	3.393	3.3910	16	4 1 1			2.1407	6	0 4 4	9	1.5573	1.5609	5	-5 7 4
11	3.276	3.2728	8	0 5 1	10	2.094	2.0864	7	-4 5 3			1.5577	3	7 1 4
9	3.215	3.2545	5	0 4 2			2.0790	2	5 2 3			1.5470	2	-3 3 6
		3.2246	3	0 1 3	9	2.050	2.0453	8	4 6 2	19	1.5296	1.5328	10	-1 10 3
		3.1893	4	-3 4 1			2.0267	2	5 5 2			1.5238	5	5 8 3
		3.1627	5	-4 0 2	4	1.9945	2.0100	2	-1 5 4			1.5198	3	1 10 3
18	3.129	3.1256	2	-3 3 2			2.0006	2	3 7 2			1.5159	2	3 1 6
		3.1040	15	-4 3 1			1.9809	2	-6 3 3	10	1.4930	1.5020	3	1 9 4
18	3.060	3.0605	11	-1 2 3	5	1.9652	1.9716	5	1 5 4			1.4884	4	-1 5 6
17	3.005	3.0113	15	5 1 0			1.9565	2	0 1 5	6	1.4698	1.4758	5	5 7 4
		2.9760	11	2 5 1	9	1.9313	1.9346	4	-4 4 4			1.4601	2	4 0 6
22	2.934	2.9311	20	2 4 2			1.9255	4	5 7 0			1.4570	2	-9 1 4
7	2.867	2.8932	3	4 0 2			1.9199	3	7 1 2			1.4458	2	6 3 5
		2.8543	4	0 3 3			1.8981	2	-5 3 4	12	1.4322	1.4342	3	6 10 0
		2.7749	2	-4 3 2	7	1.8791	1.8863	3	4 8 0			1.4272	6	0 6 6
6	2.758	2.7446	5	4 2 2			1.8743	6	0 6 4			1.4228	5	-6 9 3
18	2.728	2.7351	9	-3 2 3	8	1.8589	1.8640	2	0 3 5					
		2.7177	2	1 6 1			1.8574	2	-6 0 4					
		2.7048	11	2 6 0			1.8484	5	7 5 0					

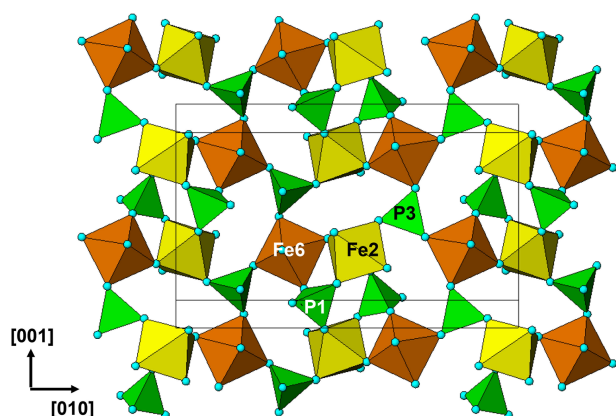


Figure 6. Heteropolyhedral {100} layer at $x = 0$ in regerite.

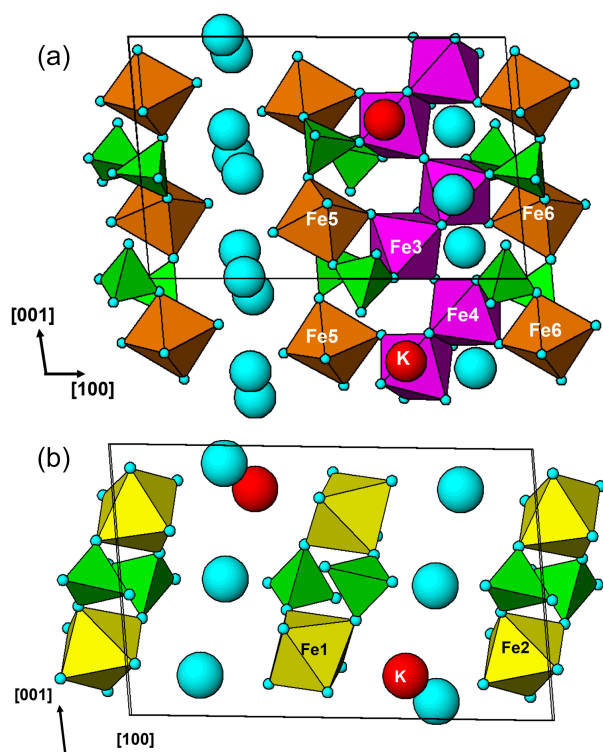


Figure 7. (a) Regerite structure, {010} slice at $y = 0.25$. (b) Regerite structure, {010} slice at $y = 0$

$c = 9.870(11) \text{ \AA}$, $\beta = 95.42(2)^\circ$, $V = 2621(3) \text{ \AA}^3$ and $Z = 4$.

Single-crystal diffraction data were collected at the Australian Synchrotron microfocus beamline MX2 (Aragao et al., 2018). Intensity data were collected using a Dectris Eiger 16M detector and monochromatic radiation with a wavelength of 0.7109 \AA . The crystal was maintained at 100 K in an open-flow nitrogen cryostream during data collections. The diffraction data were collected using a single 36 s sweep of 360° rotation around ϕ . The resulting dataset consists of

Table 3. Crystal data and structure refinement for regerite.

Ideal formula	$\text{KFe}_6(\text{PO}_4)_4(\text{OH})_7(\text{H}_2\text{O})_6 \cdot 4\text{H}_2\text{O}$
Data collection	Synchrotron microfocus MX2
Temperature	100 K
Wavelength, \AA	0.7109 (synchrotron)
Space group	$P2_1/c$
Cell parameters	$a = 15.353(3) \text{ \AA}$ $b = 17.351(4) \text{ \AA}$ $c = 9.887(2) \text{ \AA}$ $\beta = 95.26(3)^\circ$
Volume, \AA^3	$2622.7(10) \text{ \AA}^3$
Z	4
Absorption correction	Multi-scan $T_{\min} = 0.33$, $T_{\max} = 0.43$
Crystal size, mm	$0.005 \times 0.015 \times 0.035$
Theta range, $^\circ$	1.33 to 32.08
Index ranges	$-20 \leq 20$, $-24 \leq 24$, $-12 \leq 12$
Reflections collected	47223
Independent reflections	7303 [$R_{\text{int}} = 0.065$]
Reflections $I > 3\sigma(I)$	6088
Refinement method	Full-matrix, least squares on F
restraints/constraints/parameters.	34/24/473
R indices, $I > 3\sigma(I)$	$R_{\text{obs}} = 0.047$, $wR_{\text{obs}} = 0.065$
R indices, all data	$R_{\text{obs}} = 0.054$, $wR_{\text{obs}} = 0.067$
Largest ΔF peaks	$+1.06, -1.73 \text{ e} \cdot \text{ \AA}^{-3}$

3600 individual images with an approximate ϕ angle of each image being 0.1° . The raw intensity dataset was processed using XDS software to produce data files that were analysed using SHELXT (Sheldrick, 2015) and Jana2006 (Petříček et al., 2014). Refined unit-cell parameters are provided in Table 3.

6.1 Structure refinement

A structural model was obtained in space group $P2_1/c$ using SHELXT (Sheldrick, 2015) and refined using Jana2006 (Petříček et al., 2014). The model has 6 Fe atoms, 4 P atoms, 1 K atom and 33 O atoms per formula unit. After anisotropic displacement parameter refinement for all metals and oxygen atoms ($wR_{\text{obs}} = 0.076$), difference Fourier maps were used to locate 25 H atoms of a possible 27, based on the structure containing $7(\text{OH}) + 10(\text{H}_2\text{O})$. The H atoms were refined with soft restraints ($\text{O-H} = 0.85(1) \text{ \AA}$ and $\text{H-O-H} = 109.47(1)^\circ$) and with the same isotropic displacement parameter, resulting in convergence at $wR_{\text{obs}} = 0.065$ for 6088 reflections with $I > 3\sigma_I$. Other details on the data collection and refinement are given in Table 3. Refined atom

Table 4. Atom coordinates, equivalent isotropic displacement parameters (\AA^2) and bond-valence sums (BVSs) for regerite.

Atom	x	y	z	U_{eq}	BVS
Fe1	0.55318(3)	0.46994(3)	1.24646(5)	0.01035(13)	3.04
Fe2	-0.05199(3)	0.47511(3)	-0.25103(5)	0.01067(13)	3.01
Fe3	0.31905(3)	0.23659(3)	0.36126(5)	0.01260(13)	3.04
Fe4	0.16675(3)	0.25914(3)	0.13879(5)	0.01310(13)	3.07
Fe5	0.52332(3)	0.33397(3)	0.75940(5)	0.01276(13)	3.10
Fe6	-0.03968(3)	0.33441(3)	0.23663(5)	0.01262(13)	3.03
P1	0.06371(5)	0.40462(4)	0.00559(8)	0.0100(2)	4.98
P2	0.42535(5)	0.40758(5)	0.99210(8)	0.0102(2)	4.97
P3	-0.02592(5)	0.32250(4)	0.56106(9)	0.0107(2)	4.93
P4	0.51069(5)	0.32054(4)	0.43817(8)	0.0103(2)	4.97
K1	0.33912(5)	0.45164(5)	1.34081(9)	0.0253(2)	1.04
O1	0.13173(14)	0.34020(13)	0.0048(2)	0.0129(6)	1.83
O2	0.04733(14)	0.43321(13)	-0.1413(2)	0.0124(6)	1.89
O3	0.10057(14)	0.46964(13)	0.1001(2)	0.0136(6)	1.79
O4	-0.02250(14)	0.37438(13)	0.0545(2)	0.0118(6)	1.79
O5	0.35313(14)	0.34670(13)	0.9948(2)	0.0128(6)	1.79
O6	0.44578(14)	0.43776(13)	1.1373(2)	0.0118(6)	1.83
O7	0.50936(14)	0.37314(13)	0.9430(2)	0.0119(6)	1.80
O8	0.39228(14)	0.47395(13)	0.8968(2)	0.0129(6)	1.79
O9	0.07267(14)	0.31203(13)	0.5648(2)	0.0140(6)	1.83
O10	-0.06730(14)	0.27318(13)	0.6676(2)	0.0117(6)	1.73
O11	-0.06862(13)	0.30110(13)	0.4182(2)	0.0118(6)	1.77
O12	-0.04746(15)	0.40851(13)	0.5867(2)	0.0143(6)	1.73
O13	0.55429(14)	0.30197(13)	0.5802(2)	0.0116(6)	1.84
O14	0.41163(14)	0.30867(13)	0.4355(2)	0.0138(6)	1.80
O15	0.55246(14)	0.27140(13)	0.3323(2)	0.0117(6)	1.77
O16	0.52615(15)	0.40664(13)	0.4070(2)	0.0134(6)	1.72
O17	0.48969(15)	0.55760(13)	1.3131(2)	0.0136(6)	1.09
O18	0.02251(15)	0.55689(13)	-0.3112(2)	0.0140(6)	1.07
O19	0.39848(14)	0.30908(14)	0.7330(2)	0.0132(6)	1.11
O20	0.21251(14)	0.18049(13)	0.2764(2)	0.0121(6)	1.01
O21	0.27143(14)	0.31712(13)	0.2248(2)	0.0123(6)	0.98
O22*	0.24355(13)	0.21844(14)	0.0009(2)	0.0117(6)	0.98
O23	0.08699(14)	0.31052(13)	0.2682(2)	0.0131(6)	0.98
O24	0.66477(16)	0.49134(16)	1.3770(3)	0.0216(7)	0.41
O25	0.61928(14)	0.37360(13)	1.1725(2)	0.0130(6)	0.37
O26	-0.12991(15)	0.38379(13)	-0.1827(2)	0.0145(6)	0.36
O27	-0.15651(17)	0.53842(17)	-0.3689(3)	0.0241(8)	0.31
O28	0.66122(15)	0.35621(14)	0.8084(3)	0.0155(7)	0.33
O29	-0.17308(15)	0.36002(15)	0.1892(3)	0.0185(7)	0.39
O30*	0.72783(18)	0.38733(17)	1.5645(3)	0.0275(9)	0.06
O31	0.25209(14)	0.54222(16)	1.0075(2)	0.0180(8)	0.01
O32	0.82586(16)	0.54008(14)	1.3487(3)	0.0158(7)	0
O33	0.75380(17)	0.23123(16)	0.8817(3)	0.0249(8)	0
H17	0.500(3)	0.569(3)	1.395(3)	0.045(3)	
H18	0.018(4)	0.559(3)	-0.397(2)	0.045(3)	
H19	0.394(4)	0.301(3)	0.651(2)	0.045(3)	
H20	0.182(3)	0.168(3)	0.339(4)	0.045(3)	
H21	0.301(3)	0.329(3)	0.162(4)	0.045(3)	
H23	0.097(4)	0.293(3)	0.344(3)	0.045(3)	
H24a	0.7195(15)	0.487(2)	1.369(5)	0.045(3)	
H24b	0.650(3)	0.5376(14)	1.368(5)	0.045(3)	
H25a	0.602(3)	0.336(2)	1.217(4)	0.045(3)	
H25b	0.595(3)	0.372(3)	1.093(3)	0.045(3)	
H26a	-0.119(3)	0.345(2)	-0.229(4)	0.045(3)	
H26b	-0.109(3)	0.377(3)	-0.101(3)	0.045(3)	
H27a	-0.168(4)	0.4922(14)	-0.362(4)	0.045(3)	
H27b	-0.157(3)	0.551(2)	-0.451(2)	0.045(3)	
H28a	0.676(3)	0.3914(19)	0.862(4)	0.045(3)	
H28b	0.690(3)	0.3164(18)	0.831(4)	0.045(3)	
H29a	-0.190(3)	0.391(3)	0.126(4)	0.045(3)	
H29b	-0.2165(19)	0.338(3)	0.217(4)	0.045(3)	
H30a	0.769(3)	0.370(3)	1.617(4)	0.045(3)	
H31a	0.218(3)	0.5139(17)	1.047(5)	0.045(3)	
H31b	0.284(3)	0.5146(18)	0.961(5)	0.045(3)	
H32a	0.816(3)	0.5811(16)	1.324(5)	0.045(3)	
H32b	0.866(2)	0.525(2)	1.317(5)	0.045(3)	
H33a	0.740(3)	0.1864(17)	0.915(4)	0.045(3)	
H33b	0.773(3)	0.261(2)	0.946(3)	0.045(3)	

* H atoms corresponding to H22 and H30b could not be located unambiguously in difference-Fourier maps.

Table 5. Polyhedral bond lengths [\AA] for regerite.

Fe1–O6	1.967(2)	1.931(2)	1.931(2)
Fe1–O8	1.968(2)	1.976(3)	1.976(3)
Fe1–O16	2.004(2)	1.984(2)	1.984(2)
Fe1–O17	1.953(2)	1.950(2)	1.950(2)
Fe1–O24	2.082(3)	2.132(2)	2.132(2)
Fe1–O25	2.120(2)	2.190(3)	2.190(3)
avg	2.016	avg	2.027
Fe3–O5	1.995(2)	Fe4–O1	1.973(2)
Fe3–O14	1.983(2)	Fe4–O9	1.988(2)
Fe3–O19	2.002(3)	Fe4–O20	2.008(2)
Fe3–O20	2.019(2)	Fe4–O21	2.017(2)
Fe3–O21	2.031(2)	Fe4–O22	2.011(2)
Fe3–O22	2.037(2)	Fe4–O23	2.054(3)
avg	2.011	avg	2.008
Fe5–O7	1.968(2)	Fe6–O4	1.970(2)
Fe5–O13	1.956(2)	Fe6–O10	2.019(2)
Fe5–O15	2.001(2)	Fe6–O11	1.975(2)
Fe5–O17	2.017(2)	Fe6–O18	2.033(2)
Fe5–O19	1.959(2)	Fe6–O23	1.985(2)
Fe5–O28	2.163(2)	Fe6–O29	2.106(2)
avg	2.011	avg	2.014
P1–O1	1.530(2)	P2–O5	1.533(2)
P1–O2	1.533(2)	P2–O6	1.533(2)
P1–O3	1.539(2)	P2–O7	1.540(2)
P1–O4	1.542(2)	P2–O8	1.544(2)
avg	1.536	avg	1.537
P3–O9	1.522(2)	P4–O13	1.534(2)
P3–O10	1.539(2)	P4–O14	1.532(2)
P3–O11	1.547(2)	P4–O15	1.535(2)
P3–O12	1.554(2)	P4–O16	1.548(2)
avg	1.540	avg	1.537
K1–O6	2.719(3)		
K1–O14	2.842(3)		
K1–O16	2.990(3)		
K1–O17	2.986(3)		
K1–O21	2.761(3)		
K1–O24	2.966(3)		
K1–O27	2.848(3)		
K1–O30	3.149(3)		
avg	2.908		

Table 6. Hydrogen bonds in regerite.

Donor–H–acceptor	D–H (Å)	H... A (Å)	D–A (Å)	A–H... D (°)
O28–H28a–O31	0.83(4)	1.99(4)	2.783(4)	161(4)
O29–H29a–O31	0.85(4)	1.94(4)	2.774(4)	168(4)
O28–H28b–O33	0.84(4)	1.82(4)	2.657(4)	179(4)
O26–H26a–O10	0.84(4)	1.83(4)	2.657(3)	165(5)
O27–H27a–O12	0.83(3)	2.44(5)	2.866(4)	113(5)
O27–H27a–O30	0.83(3)	2.48(4)	3.201(4)	146(4)
O24–H24a–O32	0.85(3)	1.90(3)	2.653(4)	146(4)
O20–H20–O1	0.84(5)	1.88(4)	2.697(4)	165(5)
O31–H31a–O3	0.84(4)	2.07(4)	2.869(3)	159(4)
O29–H29b–O33	0.84(4)	2.10(4)	2.790(4)	139(3)
O21–H21–O5	0.83(5)	1.93(5)	2.744(4)	170(5)
O32–H32a–O20	0.76(3)	2.02(3)	2.771(3)	169(5)
O24–H24b–O17	0.84(3)	2.50(4)	2.939(4)	114(3)
O33–H33a–O30	0.88(3)	1.98(4)	2.791(4)	154(3)
O31–H31b–O8	0.84(4)	1.97(4)	2.768(3)	157(4)
O30–H30a–O26	0.84(4)	2.41(4)	3.165(4)	150(4)
O27–H27b–O32	0.84(2)	1.98(2)	2.781(4)	159(4)
O19–H19–O14	0.82(2)	2.17(3)	2.966(4)	163(5)
O25–H25a–O15	0.84(4)	1.81(4)	2.644(3)	168(4)
O25–H25b–O7	0.84(3)	1.89(4)	2.701(3)	162(4)
O26–H26b–O4	0.85(3)	1.94(4)	2.745(3)	159(5)
O32–H32b–O2	0.77(4)	2.39(4)	2.990(4)	135(4)
O32–H32b–O18	0.77(4)	2.22(4)	2.923(3)	152(4)
O18–H18–O12	0.85(2)	2.05(3)	2.849(4)	158(5)
O23–H23–O9	0.81(3)	2.27(3)	2.961(4)	143(5)
O17–H17–O16	0.84(3)	2.08(3)	2.868(4)	158(5)
O28–H28a–O31	0.83(4)	1.99(4)	2.783(4)	161(4)

coordinates, equivalent isotropic displacement parameters and bond valence sums (BVSs; Gagné and Hawthorne, 2015) are reported in Table 4. As seen from the BVS values, O1 to O16 are oxygen atoms, O17 to O23 are hydroxyls, and O18 to O33 are water molecules. Polyhedral bond distances are given in Table 5, and H-bonding is shown in Table 6. The BVS values for the sites Fe1 to Fe6 are all very close to 3, corresponding to ferric iron. The 0.45 Ti^{4+} per formula unit in the empirical formula must be relatively randomly distributed over the six Fe sites. The Ti substitution is most likely charge-balanced according to $\text{Fe}^{3+} + \text{H}_2\text{O} = \text{Ti}^{4+} + (\text{OH})^-$, with the hydroxyl ions randomly distributed over the six H_2O groups coordinated to Fe1 to Fe6 in Table 4. A band in the Raman spectrum for regerite at 805 cm^{-1} is in a similar position to bands reported for Ti-bearing paulkerrite-group minerals (Grey et al., 2023) and for titanate compounds having Ti displaced from the centres of octahedra to give a short Ti–O distance of $\sim 1.8 \text{ \AA}$ (Bamerger et al., 1990; Tu et al., 1996; Silva et al., 2018). We checked for the possibility of displaced Ti at the six Fe sites in difference Fourier maps, but the level of Ti at the sites is too low to get an unambiguous confirmation of this.

7 Discussion

Regerite has a previously unreported crystal structure. It is shown in projection along [001] in Fig. 5. It is made of heteropolyhedral layers parallel to {100} at $x = 0$ and $x = 0.5$, which are interconnected via edge-shared octahedral dimers to form slit-like channels along [001] that are occupied by K^+ ions and water molecules (O30 to O33 in Table 4). A view of the heteropolyhedral layer at $x = 0$ is shown in Fig. 6. Octahedra $\text{Fe}_2(\text{Op})_3(\text{OH})(\text{H}_2\text{O})_2$ and $\text{Fe}_6(\text{Op})_3(\text{OH})_2(\text{H}_2\text{O})$ (Op is oxygen shared with P) and tetrahedra P1O_4 and P3O_4 share corners to form 3-, 4- and 6-member rings. An analogous layer at $x = 0.5$ is formed from Fe1- and Fe5-centred octahedra and P2- and P4-centred tetrahedra.

The dimers of octahedra, centred by Fe3 and Fe4, are shown in Fig. 7a. The dimers share corners to give chains along [001]. These chains share corners with [001] chains of alternating octahedra (centred at Fe5 and Fe6) and tetrahedra to give four-octahedra-wide ribbons centred at $y = \frac{1}{4}$, as shown in Fig. 7, and $y = \frac{3}{4}$. The ribbons alternate with layers containing four-member rings of alternating Fe1- and Fe2-centred octahedra with PO_4 tetrahedra at $y = 0$ and $\frac{1}{2}$, as shown in Fig. 8.

Data availability. Crystallographic data for regerite are available in the Supplement.

Supplement. The supplement related to this article is available online at: <https://doi.org/10.5194/ejm-35-805-2023-supplement>.

Author contributions. IEG oversaw the research and wrote the paper. RH and CR provided the specimen and obtained preliminary EDS analyses. CR obtained optical images of the specimen. CMM conducted the EMP analyses. ARK measured the optical properties, Raman spectrum, PXRD and crystal morphology. SB collected the single-crystal diffraction data.

Competing interests. The contact author has declared that none of the authors has any competing interests.

Disclaimer. Publisher's note: Copernicus Publications remains neutral with regard to jurisdictional claims in published maps and institutional affiliations.

Acknowledgements. We thank Cameron Davidson for preparing a polished mount of the specimen for electron microprobe analysis. This research was undertaken in part using the MX2 beamline at the Australian Synchrotron, part of ANSTO, and made use of the Australian Cancer Research detector.

Review statement. This paper was edited by Sergey Krivovichev and reviewed by Lyudmila Lyalina and Alan Pring.

References

- Aragao, D., Aishima, J., Cherukuvada, H., Clarken, R., Clift, M., Cowieson, N. P., Ericsson, D. J., Gee, C. L., Macedo, S., Mudie, N., Panjekar, S., Price, J. R., Riboldi-Tunncliffe, A., Rostan, R., Williamson, R., and Caradoc-Davies, T. T.: MX2: a high-flux undulator microfocuss beamline serving both the chemical and macromolecular crystallography communities at the Australian Synchrotron, *J. Synchr. Radiat.*, 25, 885–891, 2018.
- Bamberger, C. E., Begun, G. M., and MacDougall, C. S.: Raman spectroscopy of potassium titanates: Their synthesis, hydrolytic reactions and thermal stability, *Appl. Spectr.*, 44, 31–37, 1990.
- Fischer, G.: Über die modale Zusammensetzung der Eruptiva im ostbayerischen Kristallin, *Geologica Bavarica*, 55, 7–23, 1965.
- Gagné, O. C. and Hawthorne, F. C.: Comprehensive derivation of bond-valence parameters for ion pairs involving oxygen, *Acta Crystallogr.*, 71, 562–578, 2015.
- Grey, I. E., Hochleitner, R., Rewitzer, C., Kampf, A. R., MacRae, C. M., Gable, R. W., Mumme, W. G., Keck, E., and Davidson, C.: Pleysteinite, $[(\text{H}_2\text{O})_{0.5}\text{K}_{0.5}]_2\text{Mn}_2\text{Al}_3(\text{PO}_4)_4\text{F}_2(\text{H}_2\text{O})_{10} \cdot 4\text{H}_2\text{O}$, the Al analogue of benyacarite, from the Hagendorf Sud pegmatite, Oberpfalz, Bavaria, Germany, *Eur. J. Mineral.*, 35, 189–197, 2023.
- Gunter, M. E., Bandli, B. R., Bloss, F. D., Evans, S. H., Su, S. C., and Weaver, R.: Results from a McCrone spindle stage short course, a new version of EXCALIBUR, and how to build a spindle stage, *Microscope*, 52, 23–39, 2004.
- Petříček, V., Dušek, M., and Palatinus, L.: Crystallographic Computing System JANA2006: General features, *Z. Krist.*, 229, 345–352, 2014.
- Sheldrick, G. M.: Crystal-structure refinement with SHELX, *Acta Crystallogr.*, 71, 3–8, 2015.
- Silva, F. L. R., Filho, A. A. A., Silva, M. B., Balzuweit, K., Banti-gnies, J.-L., Caetano, E. W. S., Moreira, R. L., Freire, V. N., and Righi, A.: Polarized raman, FTIR, and DFT study of $\text{Na}_2\text{Ti}_3\text{O}_7$ microcrystals, *J. Raman Spectr.*, 49, 535–548, 2018.
- Tu, C.-S., Guo, A. R., Tao, R., Katiyar, R. S., Guo, R., and Bhalla, A. S.: Temperature dependent Raman scattering in KTiOPO_4 and KTiOAsO_4 single crystals, *J. Appl. Phys.*, 79, 3235–3240, 1996.
- Wilk, H.: Der Quarzpegmatit von Pleystein und seine Phosphatparagenese, *Der Aufschluss, Sonderheft 16*, edited by: Metz, R., *Zur Mineralogie und Geologie der Oberpfalz*, 199–212, 1967.